Experimental report

15/09/2023

Proposal: 9-11-2095 **Council:** 10/2022

Title: In-situ observation of diffusion in layer-by-layer polyelectrolyte films

Research area: Chemistry

This proposal is a new proposal

Main proposer: Christiane A. HELM

Experimental team: Muhammad KHURRAM
Annekatrin SILL
Heiko AHRENS
Sven NEUBER

Local contacts: Philipp GUTFREUND

Samples: PEI, PSS, PDADMA, H2O, NaCl,

Instrument	Requested days	Allocated days	From	To
D17	4	3	19/06/2023	22/06/2023

Abstract:

Polyelectrolyte layer-by-layer films are prepared by sequential adsorption of oppositely charged polyelectrolytes. The films consist of a deuterated and a protonated slab prepared by selectively deuterated polyanions. Annealing in high salt solution causes interdiffusion which broadens the internal interface between the two slabs and allows for the calculation of the diffusion constant D of the polyanion. D at different annealing temperatures will be measured. Thus, the binding enthalpy between electrostatic monomer-monomer bonds can determined with an Arrhenius plot.
Additionally, we will test different surface modifications for contrast enhancement and dedicate a few experiments to film swelling in different annealing solutions. Funding is by Deutsche Forschungsgemeinschaft (SFB 1270).

Proposal 9-11-2095 In-situ observation of diffusion in layer-by-layer polyelectrolyte films

Layer-by-layer films (LbL films) are formed by sequential adsorption of oppositely charged polyelectrolytes (PEs), synthetic PEs, proteins, DNA, or nanoparticles [1]. LbL films have stimulated great interests from both academic researchers and industry due to their potential applications. Yet, it remains a challenge to control the position and mobility of the molecules within the film for selected applications such as drug delivery.

As polycations linear polydiallyldimethylammonium chloride (PDADMA) is used, polystyrene sulfonate (PSS) is the polyanion. LbL films formed at 0.1 M NaCl deposition solution is one of the standard systems [2-7]. We studied *D*(PSS), the diffusion constant of the polyanion, by using a slab architecture: the multilayer consists of selectively deuterated slabs. Previously we exposed the LbL film to an annealing solution for a defined time. Then, the film was dried and investigated by monochromatic neutron reflectometry [3, 5, 9]. To obtain a diffusion constant, LbL-films from the same batch were annealed for individual times, giving a snapshot of the frozen-in polymer movement.

Now we used a single film, annealed it in 1 M NaCl solution, and observed the polymer diffusion in situ (cf. Figure 1), employing neutron time of flight reflectometry [8]. We chose the molecular weight of PDADMA low to be below the entanglement limit [9]. The film consists of a deuterated and a protonated slab. To functionalize the silicon block, the first two layers had polyethyleneimine (PEI) as polycation. The polycation is PDADMA with M_w(PDADMA) = 35 kDa, as polyanions PSS with M_w(PSS) = 75.6 kDa and PSSd with M_w(PSSd) = 79 kDa were used. The multilayer (in total 17 bilayers) is built from deposition solutions containing 1mM/Monomer of the respective polyion and 100 mM NaCl. The resulting film thickness in air was 500 Å (confirmed by in-house XRR), swelling in 1 M NaCl led to 780 Å [8]. TOF-NR measurements in 1 M NaCl solution at 20 °C are shown in Fig. 1 at indicted annealing times.

The data were fitted with a slab model [5]. To improve the contrast and increase the intensity at large Q_z-values, a 3 nm thick PEI slab was added. Its thickness is based on the molecular structure of branched PEI with its high charge density [3 Nestler et al., 2015, 9].

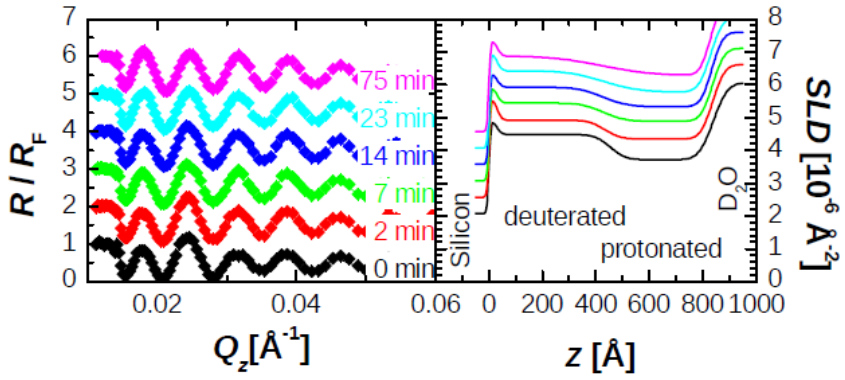

Fig. 1: In-situ annealing of a polyelectrolyte multilayer film in 1 M NaCl solution at 30 °C: neutron reflectivity curves normalized with respect to the Fresnel reflectivity R_F of an ideally flat surface (left) and corresponding SLD profiles (right). The layer sequence is $(PEI/PSSd)_2$ / $(PDADMA/PSSd)_8$ / $(PDADMA/PSS)_7$. For the SLD profiles, z = 0 is set to the interface between the silicon substrate and the deuterated slab. For clarity, both the reflectivity curves and the SLD profiles are shifted vertically. Different annealing times are indicated.

Originally, we intended to determine the diffusion constant of PSS from the widening of the internal interface between the protonated and deuterated slab over the diffusion/annealing time (cf. Figure 2) [5]. However, at high annealing temperatures, diffusion was very fast. Intermixing of the protonated and deuterated slab occurred almost immediately (cf. Fig. 3). Therefore, the diffusion constant was calculated from the time-dependent changes of the SLD of the two slabs [5].

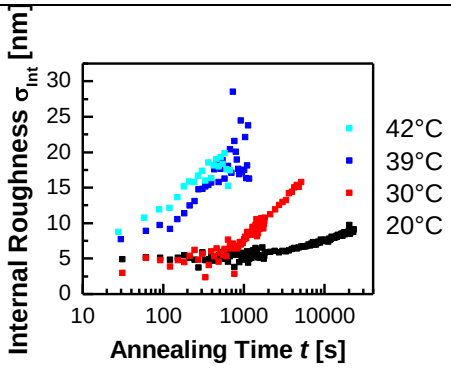

Fig. 2: Internal roughness vs annealing time t. The annealing temperature was varied as indicated.

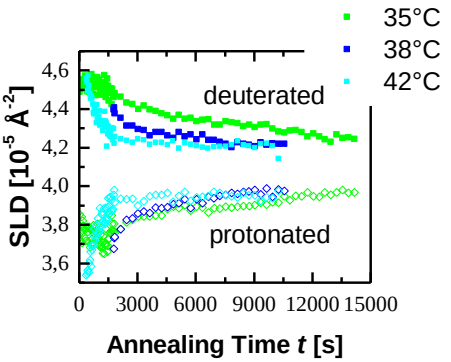

Fig. 3: SLD of the protonated and deuterated slab vs annealing time t. Annealing was performed at different temperatures as indicated.

We found that the diffusion constant of PSS increases with temperature by three orders of magnitude (from $6.4 \cdot 10^{-22}\ \mathrm{m^2/s}$ to $12\,300 \cdot 10^{-22}\ \mathrm{m^2/s}$). Therefore, the relationship between the diffusion constant D_{PSS} and the annealing temperature T can be described with the Arrhenius equation [10]: $D_{PSS} = D_0 \exp(-\frac{E_A}{R_{gas} \cdot T})$ with R_{gas} the universal gas constant and D_0 a materials parameter. The obtained activation energy $E_A = 57.3\ \mathrm{kJ/mol}$ is a factor of three smaller than the values obtained in earlier work [Sill et al., 2021]. The low activation energy is attributed to the fact that the films are below the entanglement limit.

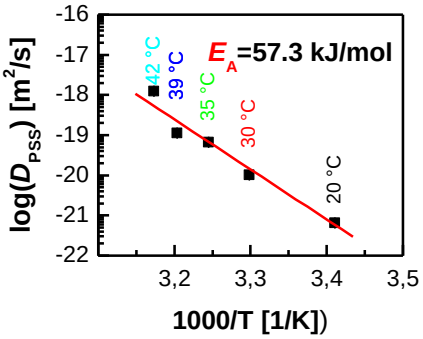

Fig. 4: Dependence of PSS diffusion constant D_{PSS} on annealing temperature and fit to the Arrhenius equation (solid line). The obtained activation energy is indicated.

References

1 Decher G, *Science* (1997) 277, 1232.; Von Klitzing R, *PCCP*, (2006) 8, 501; Costa RR, Mano JF (2014) *Chemical Reviews* 43 (2014) 3453.

2 Lavalle P, Gergely C, Cuisinier FJG, Decher G, Schaaf P, Voegel JC, Picart C. *Macromolecules* 35 (2002) 4458.

3 Nestler P, Paßvogel M, Helm CA, *Macromolecules* 46 (2013) 5622; Paßvogel M, Nestler P, Köhler R, Solltwedel O, Helm CA, *Macromolecules* 49 (2016) 935; Sill A, Nestler P, Weltmeyer A, Paßvogel M, Neuber S, Helm CA *Macromolecules* 53 (2020) 7107; Sill A, Nestler P, Thran P, Helm CA, *Macromolecules*, 54 (2021) 9372.

4 Selin V, Ankner JF, Sukhishvili SA, *Macromolecules* 48 (2015) 4983.

5 Nestler P, Paßvogel M, Ahrens H, Köhler R, Helm CA, *Macromolecules* 48 (2015) 8546; Soltwedel O, Ivanova O, Nestler P, Müller M, Köhler R, Helm CA *Macromolecules* 43 (2010) 7288.

6 Selin V, Ankner JV, Sukhishvili SA, *Macromolecules* 50 (2017) 6192.

7 Lalwani SM, Eneh CI, Lutkenhaus JK, *Physical Chemistry Chemical Physics* 22 (2020) 24157.

8 Sill A, Ahrens H, Soltwedel O, Gutfreund P, Neuber S, Nestler P, Helm CA, *ACS Macro Letters, subm.*

9 Sill A, Nestler P, Azinfar A, Helm CA, *Macromolecules*, 52 (2019) 9045.

10 Jost, W. Diffusion in Solids, Liquids, Gases; Academic Press, 1960.